Part VIII

High-Velocity Clouds, Galactic Halo Models, Observations of the LMC

https://doi.org/10.1017/S0252921100071438 Published online by Cambridge University Press

The Bavarian Evening ...

... a mixture of local culture and Spanish flair.

https://doi.org/10.1017/S0252921100071438 Published online by Cambridge University Press

High-Velocity Clouds and their Soft X-ray Emission

J. Kerp[1], J. Pietz[1], P.M.W. Kalberla[1], W.B. Burton[2], R. Egger[3], M.J. Freyberg[3], Dap Hartmann[4], and U. Mebold[1]

[1] Radioastronomisches Institut der Universität Bonn, Auf dem Hügel 71, D-53121 Bonn, Germany
[2] Sterrewacht Leiden, P.O. Box 9513, NL-2300 RA Leiden, The Netherlands
[3] Max-Planck-Institut für extraterrestrische Physik, Postfach 1603, D-85740 Garching, Germany
[4] Harvard-Smithsonian Center for Astrophysics, 60 Garden Street, Cambridge, MA 02138, U.S.A.

Abstract. Diffuse excess 1/4 keV soft X-ray emission was found to be positionally correlated with the column density distribution of the high velocity cloud (HVC) complex C (Kerp et al. 1996). Here we point out that the detected diffuse X-ray emission is indeed associated with the HVC phenomenon. For this purpose we study the 1/4 keV radiation transfer as well as the H I column density distribution of HVCs and intermediate velocity clouds (IVCs) towards HVC complex C in detail. We present evidence that on arcmin scales the 3/4 keV soft X-ray emission is positionally anticorrelated with the HVC column density distribution of an individual HVC filament of complex C.

1 Introduction

Up to now HVCs have been detected, in emission, only in the line radiation of the neutral atomic hydrogen (for a comprehensive review see Wakker & van Woerden 1997). Recent analyses of *ROSAT* data suggest that HVCs also emit soft X-rays (Herbstmeier et al. 1995 and Kerp et al. 1994, 1995, 1996). Here we focus on HVC complex C towards high galactic latitudes. We present a comparative analysis of X-ray and H I 21 cm line data available in this region ($73° \leq l \leq 118°$, $38° \leq b \leq 63°$).

In the 1/4 keV energy regime one has to disentangle the X-ray emission of the individual soft X-ray sources which contribute to the observed X-ray background in order to reveal the excess emission associated with the HVCs. Especially the intermediate- and low-velocity gas determines the intensity distribution of the soft X-ray sky, by photoelectric absorption. Because of the much smaller absorption cross section in the 3/4 keV band such a decomposition is not necessary. We will demonstrate that it is feasible to separate the emission of the "normal" soft X-ray background (SXRB) from that of the excess emission associated with HVCs. In consequence we have to solve the radiation transport of soft X-ray photons through the galactic interstellar

https://doi.org/10.1017/S0252921100071438 Published online by Cambridge University Press

medium (ISM) to identify sky areas which reveal deviations from this "normal" SXRB intensity distribution.
Here we focus on two aspects which are important to understanding the recent results on X-ray emission of HVCs. First, we will show that the *ROSAT* 1/4 keV all-sky survey data reveal soft X-ray emission which is positionally correlated with the HVCs of complex C. We show new H I 21 cm line maps of the total and IVC column density distribution and discuss the relation of the individual cloud populations to the appearance of the soft X-ray intensity distribution on the sky. Second, we will discuss in Sect. 3 the small scale positional association of an individual HVC filament with excess soft X-ray emission in the *ROSAT* 3/4 keV energy band. This is of importance because the 3/4 keV radiation can penetrate the galactic ISM without significant attenuation towards high galactic latitudes.

2 The Soft X-ray Background

It is a matter of discussion whether the SXRB has a patchy source intensity distribution or not (see also Pietz et al., Snowden, and Wang; this volume). For our purpose knowledge of the soft X-ray intensity distribution on large angular scales is vital to disclose "deviating" X-ray emission close to individual clouds.
The *ROSAT* mission established the existence of three main SXRB source components. The first one is the well known local X-ray radiation originating within the local void of neutral matter. Its radiation dominates the emission within the *ROSAT* 1/4 keV band, while it is nearly undetectable in the *ROSAT* 3/4 keV and 1.5 keV energy bands (Snowden et al. 1993).
Also well known is the radiation of the extragalactic X-ray background. The diffusely distributed extragalactic X-ray emission is the superposition of the radiation of individual, unresolved X-ray sources (Hasinger et al. 1993, Gendreau et al. 1995). The extragalactic X-ray background dominates the emission within the *ROSAT* 1.5 keV band and accounts for a large fraction of the observed 3/4 keV radiation but contributes only a few percent to the observed total 1/4 keV radiation.
Of greatest importance for the present paper is the intensity distribution of the third diffuse X-ray source, the Galactic X-ray halo. During the *ROSAT* mission it became obvious that a significant fraction of soft X-rays originate within the Galactic halo. Here we show that, consistent with the approach of Pietz et al. and Wang (both, this volume), the observational 1/4 keV and 3/4 keV X-ray data are in quantitative agreement with a *smooth* Galactic X-ray halo intensity distribution across the entire Galactic sky. This smooth Galactic X-ray halo intensity distribution together with the isotropic extragalactic background radiation gives us the opportunity to study the 1/4 keV X-ray properties of an entire HVC complex towards the high-latitude sky.

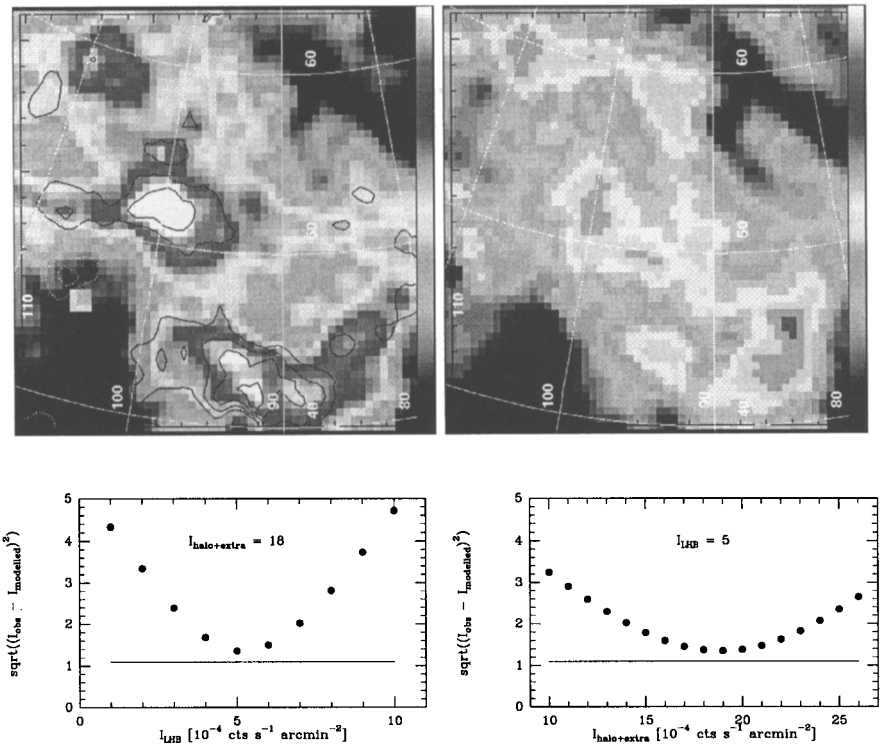

Fig. 1. *Top left:* Map extracted from the *ROSAT* 1/4 keV all-sky survey (Snowden et al. 1997) with an angular resolution of 48′. White denotes high X-ray intensities while black indicates weak X-ray emitting areas. The 1/4 keV minimum count rate displayed is $I_{1/4\,\mathrm{keV}}(\mathrm{min}) = 7 \cdot 10^{-6}\,\mathrm{cts\,s^{-1}\,arcmin^{-2}}$, the maximum displayed count rate is $I_{1/4\,\mathrm{keV}}(\mathrm{max}) = 18 \cdot 10^{-6}\,\mathrm{cts\,s^{-1}\,arcmin^{-2}}$. Superimposed as contour lines are the areas of excess emission (solid contours) and too weak X-ray emission (dashed contours). The contour levels start at 4σ and increase in steps of 2σ. *Top right:* Modelled 1/4 keV SXRB intensity distribution towards the same part of the galactic sky as shown *left*. The intensity scale is identical with that of the *left* map. To model this map we assumed $I_{\mathrm{local}} = 4.4 \cdot 10^{-6}\,\mathrm{cts\,s^{-1}\,arcmin^{-2}}$, $I_{\mathrm{halo}} = 16 \cdot 10^{-6}\,\mathrm{cts\,s^{-1}\,arcmin^{-2}}$, and $I_{\mathrm{extra}} = 2.3 \cdot 10^{-6}\,\mathrm{cts\,s^{-1}\,arcmin^{-2}}$. These SXRB source intensity values are assumed to be constant across the *entire* field of interest.
Bottom: To evaluate the statistical significance of our modelling of the 1/4 keV X-ray intensity distribution we calculated the field averaged standard deviation between the observed and modelled intensity distribution as a function of I_{local} and $I_{\mathrm{halo+extra}}$. The line marks the field averaged standard deviation of the *ROSAT* all-sky survey data.

https://doi.org/10.1017/S0252921100071438 Published online by Cambridge University Press

Figure 1 presents a comparison between the observed and modelled SXRB intensity distribution towards a large part of HVC complex C (see also Kerp et al. 1996). On the left-hand side of Fig. 1 the *ROSAT* 1/4 keV image is displayed. Superimposed on the *ROSAT* grey scale map are the 4-σ and higher contour lines of the excess emission areas. For comparison, on the right-hand side of Fig. 1 we display the modelled SXRB intensity distribution towards the same sky area. Using the Leiden/Dwingeloo H I 21 cm line survey (Hartmann & Burton 1997) we can evaluate the soft X-ray radiation transfer through the X-ray absorbing galactic ISM quantitatively traced by the neutral atomic hydrogen. The modelled soft X-ray intensity distribution matches the observed one well with the exception of the areas where the contour lines are located. The X-ray dark regions (i.e. $l \sim 105°$, $b \sim 43°$, and $l \sim 88°$, $b \sim 60°$) are positionally associated with high column density areas of IVCs and low velocity clouds (LVCs, compare also Fig. 3 *left*). To calculate an image like Fig. 1 (*right*) we integrated the H I 21 cm line emission within the velocity range $v_{\rm LSR} \in [-100; +100]\,{\rm km\,s^{-1}}$. Thus, we account for the photoelectric absorption of IVCs and LVCs. The positional distribution of the X-ray absorbing ISM, traced by neutral atomic hydrogen, across the analyzed field is displayed in Fig. 1 (*bottom panel*) and Fig. 2 (*left-hand side*). The low and intermediate velocity gas column densities are represented in this grey scale map. We used the extremely simple approach that the 1/4 keV intensity across the entire field of interest is constant for *all* three SXRB source components. The derived intensities are $I_{\rm local} = 4.4{\cdot}10^{-6}\,{\rm cts\,s^{-1}\,arcmin^{-2}}$, $I_{\rm halo} = 16{\cdot}10^{-6}\,{\rm cts\,s^{-1}\,arcmin^{-2}}$ and $I_{\rm extra} = 2.3{\cdot}10^{-6}\,{\rm cts\,s^{-1}\,arcmin^{-2}}$ (Barber et al. 1996) and constant across the field of interest. The Galactic X-ray halo is the brightest X-ray source of all. That this simple assumption fits the observation well is demonstrated in Fig. 2 (*right*); here we plotted the 1/4 keV SXRB intensity distribution profiles averaged in galactic longitude and/or latitude. The dots with the corresponding 1 σ errorbars represent the observational X-ray data while the solid line, in each panel, marks the modelled SXRB intensity profile. These averaged intensity profiles indicate that our approach of constant intensities of the three source components fits the observed situation very well. We subtracted the modelled map (Fig. 1 *right*) from the observed SXRB intensity distribution (Fig. 1 *left*) to search for excess X-ray emission areas and evaluated the residuals in units of the statistical significance of the X-ray data. The contour lines start at a significance level of 4σ and increase in steps of 2σ. In absolute values 4σ is equivalent to a count rate of $I_{1/4\,{\rm keV}}(4\sigma) \simeq 4 \cdot 10^{-4}\,{\rm cts\,s^{-1}\,arcmin^{-2}}$. With respect to an averaged observed X-ray intensity of $I_{1/4\,{\rm keV}}({\rm mean}) \simeq 12 \cdot 10^{-4}\,{\rm cts\,s^{-1}\,arcmin^{-2}}$ the brightest excess emission area at $l \sim 90°$, $b \sim 42°$ is two times brighter than the "normal" SXRB intensity.

We note that the H I 21 cm line emission includes the IVCs and LVCs as absorbers of soft X-ray photons but *not* the HVCs. We *exclude* the HVC as soft

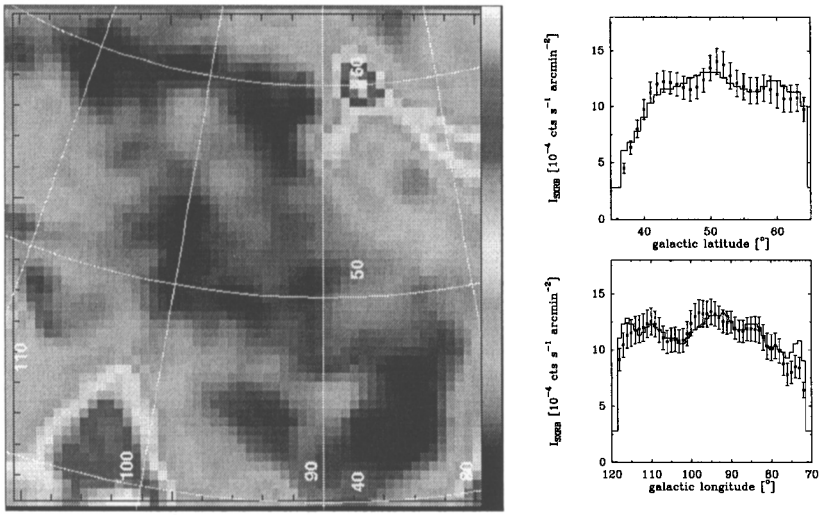

Fig. 2. *Left:* Neutral atomic hydrogen column density distribution derived from the Leiden/Dwingeloo H I 21 cm line survey (Hartmann & Burton 1997). The intensity scale is the same as in Fig. 1 with $N_{\rm HI}(\rm min) = 0.5{\cdot}10^{20}\,\rm cm^{-2}$ and $N_{\rm HI}(\rm max) = 2.0{\cdot}10^{20}\,\rm cm^{-2}$ The brightness temperature is integrated across the velocity interval of $v_{\rm LSR} \in [-100; +100]\,\rm km\,s^{-1}$. This map traces the distribution of the X-ray absorbing ISM. *Right:* Comparison of SXRB intensity profiles versus galactic coordinates averaged in galactic longitude and/or latitude. The dots with the corresponding 1 σ errorbars mark the observational data while the solid line in each panel marks the modelled SXRB intensity distribution (compare also Fig. 1 *right*). Obviously both intensity profiles match the observational data well and consequently the complex intensity pattern of the SXRB is entirely caused by photoelectric absorption because all X-ray source terms have a *constant* intensity across the field of interest.

X-ray absorbers; thus, at the position of the HVCs, our modelled SXRB map predicts a higher modelled X-ray intensity than we would obtain if the HVCs attenuate the Galactic X-ray halo emission also. Thus, our bias is towards the *non-detection* of HVC excess emission.

In Fig. 3 we compare the positional correlation of the column density distribution of the IVCs ($v_{\rm LSR} \in [-90; -25]\,\rm km\,s^{-1}$, Fig. 3 *left*) and the HVCs ($v_{\rm LSR} \in [-450; -90]\,\rm km\,s^{-1}$, Fig. 3 *right*) with the X-ray excess regions superimposed as contours on the corresponding grey scale maps. Obviously, the IVCs are not close positionally correlated to the excess X-ray emission regions, while the HVCs are nearby these areas of enhanced X-ray radiation. Especially, the area of $l \sim 90°$ and $b \sim 42°$ reveals positional correlation of the HVCs with excess X-ray emission. In Sect. 3 we will study this region using a pointed *ROSAT* observation and show that this area is also bright in 3/4 keV X-ray radiation. Because of the very different absorption cross sec-

https://doi.org/10.1017/S0252921100071438 Published online by Cambridge University Press

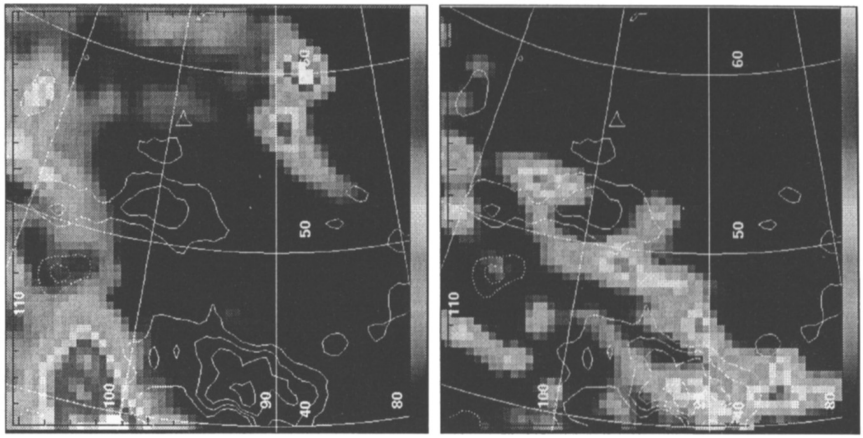

Fig. 3. *Left:* H I column density distribution of the IVCs across the field of interest. White denotes high H I column densities while black denotes low ones, with $N_{\rm HI}(\rm min) = 0.2 \cdot 10^{20}\,\rm cm^{-2}$ and $N_{\rm HI}(\rm max) = 2.0 \cdot 10^{20}\,\rm cm^{-2}$. The H I 21 cm line emission is integrated across the velocity interval $v_{\rm LSR} \in [-90; -25]\,\rm km\,s^{-1}$. The contour lines mark the 1/4 keV excess emission (solid lines) starting at the 4-σ level with steps of 2σ. *Right:* The HVC column density distribution with $N_{\rm HI}(\rm min) = 0.1 \cdot 10^{20}\,\rm cm^{-2}$ and $N_{\rm HI}(\rm max) = 1.0 \cdot 10^{20}\,\rm cm^{-2}$. The column density is derived within the velocity interval $v_{\rm LSR} \in [-450; -90]\,\rm km\,s^{-1}$; (see Plate 2).

tion of both energy bands this positional correlation demonstrates the quality of the performed radiation transfer calculation.
In conclusion, the close positional correlation between the HVCs of complex C and the excess X-ray emission region of the 1/4 keV *ROSAT* all-sky survey suggests that the HVCs are physically related to this soft X-ray enhancements.

3 The X-ray Emission of an Individual HVC Filament

The previous Section pointed out that we find a large scale positional correlation between 1/4 keV X-ray emission and the H I column density distribution of HVC complex C. Now we will demonstrate that HVCs reveal a detailed positional anticorrelation of H I column density distribution and 3/4 keV emission. This is of importance because the photoelectric absorption cross section of the galactic ISM is a factor of 10 lower in the 3/4 keV band than in the 1/4 keV range. For instance, the effective photoelectric 3/4 keV absorption cross section is $\sigma(\rm N_{HI} = 1.5 \cdot 10^{20}\,cm^{-2}) = 9 \cdot 10^{-22}\,cm^2$. This H I column density which is typically for the *warm neutral medium* (WNM) towards the northern galactic sky. It attenuates the distant 3/4 keV X-ray emission by only 13%. Here we study an HVC filament belonging to the HVC complex C

https://doi.org/10.1017/S0252921100071438 Published online by Cambridge University Press

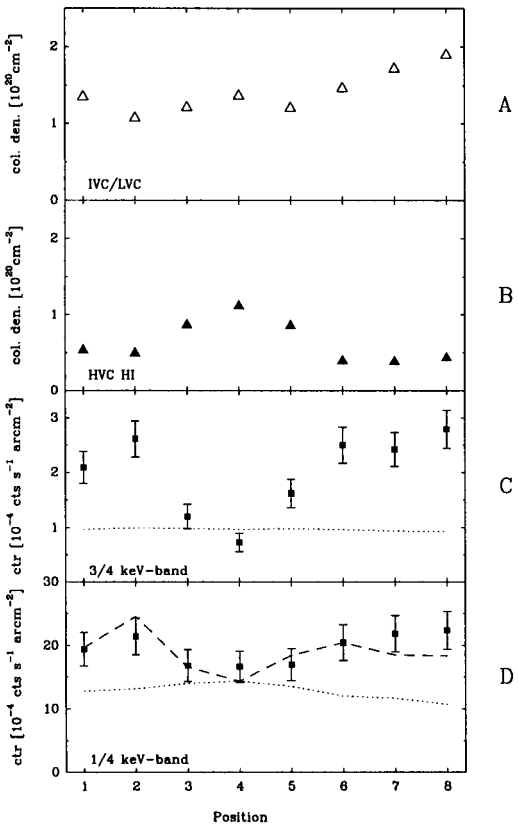

Fig. 4. Diagram showing the functional dependence of IVC/LVC and HVC column density as well as the *ROSAT* 3/4 keV and 1/4 keV count rate on positions along a linear slice across HVC 90.5+42.5–130 (see Fig. 1 of Kerp et al. 1994). The "normal" 3/4 keV and 1/4 keV SXRB intensity level is marked by the dotted line in the corresponding panel. In panel D (1/4 keV emission) the dashed line represents the modelled count rate applying the working hypothesis that the 3/4 keV excess plasma radiation produces also 1/4 keV emission. This constrains also the plasma temperature responsible for the HVC excess X-ray radiation to about $T \simeq 10^{6.2-6.3}$ K. A detailed discussion of this figure can be found in the text below.

and denoted as HVC 90.5+42.5–130 (Kerp et al. 1994, 1995). This filament has also an H I column density of $N_{\rm HI} = 1.2 \cdot 10^{20}\,{\rm cm}^{-2}$. Figure 4 shows a linear slice of 2° extent across the HVC 90.5+42.5–130 (compare also Fig. 1 of Kerp et al. 1994). In panel A the IVC/LVC column density is plotted as function of the position along the linear slice. This gas traces quantitatively the photoelectric absorption as discussed in Sect. 2. Panel B displays the HVC column density distribution along the linear slice. The peak column density

https://doi.org/10.1017/S0252921100071438 Published online by Cambridge University Press

is about $N_{\rm HI}({\rm HVC}) \simeq 1.2 \cdot 10^{20} {\rm cm}^{-2}$. The sum of the IVC/LVC and the HVC column density is about $N_{\rm HI}({\rm total}) \simeq 2.7 \cdot 10^{20}\,{\rm cm}^{-2}$ at the maximum. Panel C shows the *ROSAT* 3/4 keV intensity along this slice. A strong anticorrelation between the HVC column density and the 3/4 keV emission is detected.

Next we evaluate whether or not this obvious anticorrelation is caused by photoelectric absorption. If we sum the X-ray absorption of the WNM and the HVC filament we expect to detect a $\sim$ 26% intensity variation in the *ROSAT* 3/4 keV data. The HVC may be so distant (Wakker & van Woerden 1997) that its column density distribution only attenuates the extragalactic background radiation with an intensity of $I_{\rm extra}(3/4\,{\rm keV}) \simeq 0.53 \cdot 10^{-4}\,{\rm cts\,s^{-1}\,arcmin^{-2}}$ (Barber et al. 1996). This gives a 3/4 keV intensity attenuation of $\Delta I_{\rm extra}({\rm WNM + HVC}) = 0.10 \cdot 10^{-4}\,{\rm cts\,s^{-1}\,arcmin^{-2}}$ which is extremely difficult to detect significantly, even in deep pointed PSPC observations. If the HVCs are in front of a part of the Galactic X-ray halo, the depth of the 3/4 keV X-ray shadow increases correspondingly to the increasing amount of X-ray emitting plasma beyond the HVC. In the extreme case, all Galactic X-ray halo emission originates beyond the HVCs, the 3/4 keV radiation will be absorbed by the WNM and the HVC by $\Delta I_{\rm extra\,+\,halo}({\rm WNM + HVC}) = 0.44 \cdot 10^{-4}\,{\rm cts\,s^{-1}\,arcmin^{-2}}$ while the expected 3/4 keV intensity variation between ON and OFF the HVC is only about $\Delta I_{\rm OFF-ON} = 0.24 \cdot 10^{-4}\,{\rm cts\,s^{-1}\,arcmin^{-2}}$. But in any case the WNM absorbs the distant SXRB sources. In consequence, we do not expect to detect any significant 3/4 keV intensity variation towards the high galactic latitude sky.

But we observe three times more 3/4 keV emission close to the HVCs as radiated from the "normal" 3/4 keV X-ray background. The expected 3/4 keV intensity variation, caused by photoelectric absorption of the Galactic X-ray halo and the extragalactic background radiation by the total H I column density along the line of sight, is marked by the dotted line in panel C. The deviation between the "normal" 3/4 keV SXRB emission and the observational data yields the conclusion that we detected *excess* 3/4 keV emission. The excess 3/4 keV intensity is about a factor of two brighter than the "normal" 3/4 keV SXRB intensity variation, and a factor of about 10 larger than the expected intensity contrast even in the extreme case that the HVC is located in front of the entire Galactic X-ray halo emission.

Panel D shows the 1/4 keV intensity distribution along the linear slice. We see a similar intensity variation with position as detected in the 3/4 keV band. Here we have to account for the significant photoelectric absorption quantitatively traced by the IVC/LVC column density distribution, plotted in panel A. Again, the dotted line represents the "normal" 1/4 keV SXRB intensity distribution derived with the identical intensity values as used in Sect. 2. The low H I column density contrast along the analyzed slice yields also a low 1/4 keV intensity contrast. If we assume that the HVC rims are X-ray bright and transform quantitatively the 3/4 keV excess X-ray radiation to

the 1/4 keV energy regime, we predict a 1/4 keV intensity variation which is marked by the dashed line. This dashed line represents the observed 1/4 keV intensity variation well, suggesting that also the excess 1/4 keV emission is caused by the *same* plasma as the 3/4 keV excess emission close to the HVC. To perform this transformation $I_{3/4\,\mathrm{keV}} \rightarrow I_{1/4\,\mathrm{keV}}$ we subtracted the "normal" 3/4 keV intensity level of $I_{3/4\,\mathrm{keV}} \simeq 1.0 \cdot 10^{-4}\,\mathrm{cts\,s^{-1}\,arcmin^{-2}}$ from the individual data points along the slice and transformed the excess intensity to the *ROSAT* 1/4 keV band response. This excess 1/4 keV emission is attenuated by the IVC/LVC column density distribution shown in the lowest panel. Because the unabsorbed $I_{3/4\,\mathrm{keV}} : I_{1/4\,\mathrm{keV}}$ ratio is a very sensitive function of the plasma temperature, it varies between $I_{3/4\,\mathrm{keV}} : I_{1/4\,\mathrm{keV}} \Leftrightarrow 1 : 90$ for $T = 10^{6.0}\,\mathrm{K}$ and $I_{3/4\,\mathrm{keV}} : I_{1/4\,\mathrm{keV}} \Leftrightarrow 1 : 7$ for $T = 10^{6.3}\,\mathrm{K}$, we can constrain the plasma temperature range. We find a plasma temperature of about $T \simeq 10^{6.2-6.3}\,\mathrm{K}$ for the excess X-ray emission.

In summary, we find a detailed positional anticorrelation of 3/4 keV X-ray radiation with the H I column density distribution of HVC 90.5+42.5-130. This detailed negative correlation *cannot* be caused by photoelectric absorption, because the involved column densities are more than an order of magnitude too low for a significant attenuation of the 3/4 keV radiation. In absolute numbers, the observed 3/4 keV radiation is a factor of two brighter than the "normal" 3/4 keV SXRB radiation, and the observed 3/4 keV intensity contrast is a factor of 10 higher than expected by photoelectric absorption. These are clear indications that the detailed positional anticorrelation between the HVC column density distribution and the 3/4 keV radiation is caused by *excess* X-ray emission close to the HVC. Also in the *ROSAT* 1/4 keV energy band we find excess emission. This excess 1/4 keV emission can be quantitatively evaluated from the excess 3/4 keV emission using a plasma temperature of $T \simeq 10^{6.2-6.3}\,\mathrm{K}$ close to the HVCs.

4 Summary and Conclusion

The aim of the paper was to demonstrate that HVCs are emitters of soft X-rays. In Sect. 2 we analyzed the 1/4 keV SXRB intensity distribution towards the major part of HVC complex C. We showed that the 1/4 keV SXRB intensity distribution can be modelled well by a simple soft X-ray radiation transport approach, which assumes that across the entire field of interest the local, the Galactic X-ray halo, and the extragalactic component of the 1/4 keV radiation are constant. The success of modelling the observed SXRB intensity pattern indicates that the complex SXRB brightness distribution is due to photoelectric absorption of the galactic ISM, which is quantitatively traced by the neutral atomic hydrogen. The areas of excess emission are located close to the peaks of the HVC column density distribution.

In Sect. 3 we presented evidence that on arcmin angular scales the H I column

https://doi.org/10.1017/S0252921100071438 Published online by Cambridge University Press

density distribution of a HVC is positionally anticorrelated to the 3/4 keV emission. We showed that this emission can only be interpreted in terms of excess 3/4 keV emission close to the rims of the HVC. Assuming that plasma emission is the source of the soft X-ray radiation we find that we can model also the observed 1/4 keV excess emission using a plasma temperature of $T \simeq 10^{6.2-6.3}$ K.

Using the plasma temperature and the 3/4 keV excess emission intensity we derive an emission measure of $EM_{\rm HVC} \simeq 0.015\,{\rm cm}^{-6}\,{\rm pc}$. Assuming a distance to HVC 90.5+42.5-130 of roughly 4 kpc, we find an electron density of $n_{\rm e} \simeq 0.02\,{\rm cm}^{-3}$. This is roughly a factor of ten larger than the Galactic halo density expected at this distance from the Galactic plane (Kalberla et al., this volume). This indicates that the X-ray emission close to the HVCs originates not from the heated neighbourhood of the HVC. The HVC matter itself is heated up.

Kerp et al. (1997) show that soft X-ray enhancements in the 1/4 keV and 3/4 keV energy regime are not only associated with the here presented HVC complex C. They found excess emission towards the HVC complexes D, GCN, A, and the Magellanic Stream. Moreover, they verified that the entire HVC complex C is associated with soft X-ray emission.

These findings are independently confirmed by Pietz et al. (1997) while focussing their view onto the intensity distribution of the 3/4 keV and 1/4 keV SXRB. Their difference maps, observed minus modelled SXRB intensity distribution, reveal excess emission just at the position of the HVC complexes mentioned above.

References

Barber C.R., Roberts T.P., & Warwick R.S. (1996), MNRAS 282, 157
Gendreau K.C. et al. (1995): PASJ 47, 5
Hartmann Dap, & Burton W.B. (1997): "Atlas of Galactic Neutral Hydrogen" Cambridge University Press
Hasinger G. et al. (1993): A&A 275, 1
Herbstmeier et al. (1995): A&A 298, 606
Kerp J. et al. (1997): A&A submitted
Kerp J., Lesch H., & Mack K.-H. (1994): A&A 286, L13
Kerp J., Lesch H., Mack K.-H., & Pietz J. (1995): Adv. in Space Res. Vol. 16, No. 3, 119
Kerp J. et al. (1996): A&A 312, 67
Kuntz K., & Danly L. (1996): ApJ 457, 703
Pietz J. et al. (1997): A&A, submitted
Snowden S.L., McCammon D., & Verter F. (1993): ApJ 409, L21
Snowden S.L. et al. (1997): ApJ 485, in press
Wakker B.P., & van Woerden H. (1997): ARA&A, in press